Research Article

Received: 29 August 2023 Revised: 16 October 2023 Accepted article published: 31 October 2023 Published online in Wiley Online Library:

(wileyonlinelibrary.com) DOI 10.1002/ps.7861

Chitosan- and gallic acid-based (NPF) displayed antibacterial activity against three *Pseudomonas spp.* plant pathogens and boosted systemic acquired resistance in kiwifruit and olive plants

Sara Francesconi,[a*] Vincenzo Tagliavento,[b] Serena Ciarroni,[b] Francesco Sestili[a] and Giorgio M Balestra[a]

Abstract

BACKGROUD: *Pseudomonas syringae* pv. *actinidiae* (Psa), *P. syringae* pv. *tomato* (Pst) and *P. savastanoi* pv. *savastanoi* (Psav) are bacterial plant pathogens with worldwide impact that are mainly managed by the preventive application of cupric salts. These are dangerous for ecosystems and have favoured the selection of resistant strains, so they are candidates to be replaced in the next few years. Thus, there is an urgent need to find efficient and bio-based solutions to mitigate these bacterial plant diseases. Nanotechnology could represent an innovative way to control plant diseases, providing alternative solutions to the agrochemicals traditionally employed, thanks to the formulation of the so-called third-generation and nanotechnology-based agrochemicals.

RESULTS: In this work, a novel nanostructured formulation (NPF) composed of cellulose nanocrystals (CNC) as carrier, high amylose starch (HAS) as excipient, and chitosan (CH) and gallic acid (GA) as antimicrobials, was tested at 2% *in vitro* and *in vivo* with respect to the three different *Pseudomonas* plant pathogens. *In vitro* agar assays demonstrated that the NPF inhibited ≤80% Psa, Pst and Psav. Moreover, the NPF did not decrease biofilm synthesis and it did not influence bacterial cells flocculation and adhesion. On plants, the NPF displayed complete biocompatibility and boosted the transcript levels of the major systemic acquired resistance responsive genes in kiwifruit and olive plants.

CONCLUSION: This works provides novel and valuable information regarding the several modes-of-action of the novel NPF, which could potentially be useful to mitigate Psa, Pst and Psav infections even in organic agriculture.

Supporting information may be found in the online version of this article.

Keywords: nanotechnology; chitosan; gallic acid; cellulose nanocrystals; starch; circular economy

1 INTRODUCTION

The *Pseudomonas* genus is distributed worldwide and causes an array of diseases in plants. Three *Pseudomonas* spp. are of particular concern causing severe diseases in kiwifruit, tomato and olive plants. The kiwifruit bacterial canker is caused by *P. syringae* pv. *actinidiae* (Psa), causing brown leaf spots surrounded by a chlorotic halo. The disease affects floral buds and translucent exudates appear on healthy tissues.[1] In Italy, a Psa outbreak in 2008 caused around €2 million losses with strong socioeconomic and environmental impacts.[2,3] Tomato is challenged by the bacterial speck disease, caused by *P. syringae* pv. *tomato* (Pst).[4] Symptoms involve angular spots on leaves, which can further converge, assuming a dark colour surrounded by a chlorotic halo, leading to a loss of photosynthetic efficiency in green organs. Bacterial speck outbreaks may cause ≤75% of yield losses in cases of early and severe infections.[4,5] Olive knot caused by *P. savastanoi* pv. *savastanoi* (Psav) is widely distributed in Mediterranean areas, affecting young woody organs, branches and fruits. Symptoms occur as hyperplastic outgrowths (knots) after the bacteria have indirectly penetrated by wounding.[6] Olive knot is a chronic disease, because its symptoms persist and recur for many years,

* *Correspondence to: S Francesconi, Department of Agriculture and Forest Sciences (DAFNE), University of Tuscia, Via San Camillo de Lellis, snc, Viterbo 01100, Italy. E-mail: francesconi.s@unitus.it (Francesconi)*

a *Department of Agriculture and Forest Sciences (DAFNE), University of Tuscia, Viterbo, Italy*

b *Phytoparasites Diagnostics (PhyDia) s.r.l., Viterbo, Italy*

and can lead to severe damage resulting in reduced productivity.[7] A recent study characterized the genome of the levan-positive strain PVFi1 isolated in Central Italy, which was unexpectedly identified during an epidemiological survey.[8]

The *Pseudomonas* diseases are managed by the preventive application of cupric salts.[9,10] Despite their ease of use and affordability, the use of cupric salts has been restricted by executive regulation 2018/1981, in line with the European Green Deal, which aims to reduce the use and risk of chemical pesticides by 50% by 2030. Such restrictions are linked to great concerns regarding the massive usage of cupric salts, such as phytotoxicity, selection of resistant pathogen strains, effect on nontarget organisms and ecosystem contamination.[5,10–13] Thus, cupric salts need to be replaced by a novel generation of agrochemicals (third generation), characterized by biocompatibility and sustainability. Naturally derived nanomaterials, such as cellulose nanocrystals (CNC), are characterized by no cytotoxicity and high presence of hydroxyl groups, which can be exploited to link active antimicrobial compounds.[14] CNC can provide a better coverage when applied on crops, enhance antimicrobial properties of the delivered active compound as much as control its release along time, thus concretizing the possibility to minimize the agrochemicals employed for disease control.[15] Additives also are a fundamental part of a formulation. Starch-based polymers are already well-studied as they can facilitate the hydrosolubility of molecules.[16–18] High-amylose starch (HAS) displays film-forming ability and higher gelling strength compared to conventional starch and can contribute to modulate the release of active principles in crops,[19] which can be antibacterial or elicitor-like. Indeed, innate immunity in plants can be boosted by the application of many kinds of compounds that are able to activate plant systemic defences. As an example, recent research demonstrated that the application of acibenzolar-*s*-methyl on kiwifruit plants activated the salicylic acid defence pathway genes (*PR1*, *PR2* and *PR5*).[20] Natural compounds also can act as elicitor molecules, such as chitosan (CH), which mimics fungal attacks on plants, or gallic acid (GA), a polyphenolic compound produced by plants as secondary metabolite with broad range of antibacterial properties.[21] CNC and HA starches already have been employed to fabricate a novel nanostructured particle formulation (NPF) composed of CH and GA as active antifungal compounds, which demonstrated great potential for the control of *Fusarium graminearum* and *culmorum* as much as biocompatibility and elicitor-like properties on wheat.[22,23] Given the clear evidence regarding the antifungal properties of such NPF being reported, the aim of the present research was to investigate its antibacterial potentialities against Pst, Psa and Psav, as well as as its biocompatibility and elicitor-like properties on tomato, kiwifruit and olive plants.

2 MATERIALS AND METHODS

2.1 Bacterial strains, chemicals and plant materials

The virulent bacterial strains Psa CFBP7286 (causal agent of kiwifruit bacterial canker), Pst CFBP1323 (causal agent of tomato bacterial speck) and Psav PvBa206 (causal agent of olive knot) were the reference strains. CNC and HAS used for an *in vitro* microtitre plate assay and to assemble the NPF were extracted and characterized as described in previous studies.[22,23] CH hydrochloride (99% purity, molecular weight 60 kDa, degree of deacetylation 80–90%, CAS number 70694-72-3; Merck, Darmstadt, Germany) and GA (>97% purity, CAS number 149-91-7; Merck) are the active molecules tested *in vitro* for their minimum inhibitory concentration (MIC), in order to individualize the concentrations to assemble the NPF. The NPF was composed of CNC, HAS, CH (25% w/w) and GA (2.5% w/w); this was obtained and characterized in a previous study[22] and employed at 2% (w/v) in order to have CH at 0.5% (w/v) and GA at 0.05% (w/v). Copper hydroxide ($Cu(OH)_2$, 94% purity; CAS number 20427-59-2; Alfa Aesar/Thermo Fisher Scientific, Waltham, MA, USA) was used as reference bactericidal at the suggested field dose from commercial formulations (0.1% w/v). Plants of *Actinidia deliciosa* var. Hayward, *Solanum lycopersicum* var. San Marzano and *Olea europea* var. Frantoio were employed for *in vivo* assays and grown in a climatic chamber at 24/15 °C day/-night, with 12–14 h light and 60% relative humidity.

2.2 *In vitro* antibacterial assays

2.2.1 *CNC, HAS, CH and GA MIC by 96-microtitre plate assay*

A 96-microtitre plate assay was conducted to evaluate the antibacterial activity of CNC, HAS, CH and GA at seven different concentrations (0.001, 0.005, 0.01, 0.05, 0.1, 0.5 and 1% w/v) in order to assess the MIC and to individualize the CH and GA concentrations to be employed in the assemblage of the NPF. The same assay was repeated to evaluate the synergistic antibacterial activity of CH and GA at the chosen concentrations (0.5% and 0.05%, respectively). Fresh culture of Psa, Pst and Psav were obtained by subculturing colonies on King B (KB) medium[24] at 27 °C for 48 h. The fresh single colony was gently scraped and cultured on KB broth at 27 °C for 12 h. The experiment was run in 96-microtitre plates by inoculating 1 µL bacterial suspension in 199 µL KB broth incorporated with 50 µL CNC, HAS, CH, GA or CH + GA at the previously cited concentrations, and sterilized through a syringe filter with a 0.2-µm pore size. The plates were incubated at 27 °C for 48 h. After that, the absorbance of the bacterial biomass was measured at OD_{600} by using a DR-200B Microplate reader (Diatek instruments, Wuxi City, China). Mock (untreated bacterial suspension cultured on KB medium) and blank (KB medium supplemented with CNC, HAS, CH, GA or CH + GA at the corresponding concentrations, or only KB medium) controls also were included.[25] Data were obtained from three independent experiments, each one consisting of four replicates.

2.2.2 *NPF antibacterial activity by the 96-microtitre plate assay*

The 96-microtitre plate assay was conducted to monitor bacterial biomass growth and biofilm biosynthesis in broth medium. Fresh bacterial suspension and sterilized NPF and $Cu(OH)_2$ solutions were prepared as described in the Section 2.2.1. The experiment was run in 96-microtitre plates by inoculating 1 µL bacterial suspension in 199 µL KB broth incorporated with 50 µL NPF at 2% or $Cu(OH)_2$ at 0.1%. The plates were incubated at 27 °C for 48 h. After that, the absorbance of the bacterial biomass was measured at OD_{600} by using a DR-200B microplate reader (Diatek, Kolkata, India). After that, the 250 µL suspension was gently removed from each well by using a pipette. Each well was gently washed three times with sterilized distilled water and 250 µL crystal violet at 0.1% (v/v) were pipetted into each well and incubated for 20 min at room temperature (RT). After that, the crystal violet was gently removed, each well was washed once with sterilized distilled water and left to dry at RT. Finally, 200 µL pure ethanol were added to each well and the plates were incubated for 20 min at RT. The absorbance of biosynthesized biofilm was measured at OD_{590} by using a DR-200B microplate reader (Diatek). Mock (untreated bacterial suspension cultured on KB medium) and blank (KB medium supplemented with the NPF, $Cu(OH)_2$ or only KB medium for biomass monitoring and only pure ethanol for biofilm monitoring) controls also were included.[25] Data were

obtained from three independent experiments, each one consisting of four replicates.

2.2.3 NPF antibacterial activity by the incorporated medium assay

Sterile KB was supplemented with the NPF at 2% or $Cu(OH)_2$ at 0.1%. The KB incorporated with the compounds was poured on Petri dishes and allowed to solidify. Then, a 5-mm sterile disc paper was placed at the centre of the Petri dishes and 100 µL bacterial suspension containing 1×10^6 CFU/mL (OD_{600}) were pipetted and cultured at 27 °C for 48 h. Mock control also was included. After 48 h, the bacterial growth was evaluated by measuring four bacterial colony diameters from each plate. Data were obtained from three independent experiments, each one consisting of four replicates.

2.2.4 NPF antibacterial activity by cellular aggregation assay

The aggregation assay was performed to evaluate the ability of the NPF to influence the cell-to-cell adhesion. The assay was performed using a standard protocol already present in literature.[26] Fresh bacterial suspension and sterilized NPF and $Cu(OH)_2$ solutions were prepared as described in the Section 2.2.1. The obtained solutions were pipetted into the microtitre plates and the bacterial suspension was added to each well in order to obtain a final concentration of 1×10^6 CFU/mL. The plates were incubated at 27 °C in the dark, and the absorbance from the bacterial biomass was measured at 0, 24, 48, and 72 h postincubation at OD_{600} by using a DR-200B microplate reader (Diatek). Mock (untreated bacterial suspension in sterile distilled water) and blank (sterile distilled water supplemented with the NPF, sterile distilled water supplemented with $Cu(OH)_2$, and only sterile distilled water) controls also were included. Higher absorbance values compared to the mock control were associated with more aggregated bacterial cells. Data were obtained from three independent experiments, each one consisting of four replicates.

2.2.5 NPF antibacterial activity by cellular adhesion assay

The adhesion assay was performed to evaluate the ability of the NPF to inhibit bacterial cell adhesion to the host tissue. The assay was performed following a protocol already published with some modifications.[27] Fresh bacterial suspension and sterilized NPF and $Cu(OH)_2$ solutions were prepared as described in the Section 2.2.1. The obtained solutions were pipetted into the microtitre plates and dried at 60 °C for 24 h in order to favour the adhesion of the active compounds to the plastic surface. After that, 200 µL of 1×10^6 CFU/mL suspension were pipetted into each well and incubated at 27 °C for 3 h. At the end of the incubation time, the bacterial suspension was removed with a pipette and 200 µL sterile distilled water was added to each well. The microtitre plates were bath-sonicated for 15 min to release the bacterial cells attached to the plastic surface. The 1:100 dilution from the sonicated suspension was pipetted into new microtiter plates containing 200 µL LB and incubated at 27 °C for 24 h. The absorbance from the bacterial biomass was measured at OD_{600} by using a DR-200B microplate reader (Diatek). Mock (untreated bacterial suspension cultured on LB) and blank (LB) controls also were included. Higher absorbance values compared to the mock control were associated with more adhered bacterial cells. Data were obtained from three independent experiments, each one consisting of four replicates.

2.3 *In vivo* biocompatibility assay and disease monitoring

Plantlets of kiwifruit (10-leaf stage), tomato (10-leaf stage) and olive (50 cm high, monocaule) were sprayed with the NPF or $Cu(OH)_2$ (wetted until runoff) at the previously cited concentrations. At 48 h post-treatments, kiwifruit and tomato leaves and olive branches and leaves were gently scraped with an abrasive surface to create natural openings to allow bacterial penetration. After that, plants were artificially inoculated with a bacterial suspension of 1×10^6 CFU/mL (wetted until runoff) of each pathogen on its own host. The biocompatibility of the treatments was assessed by measuring the nitrogen balance index (NBI), related to the chlorophyll and flavonoid ratio, by means of DUALEX Scientific+™ at 21 days after the treatments. The NBI was measured by positioning the instruments in the centre of the leaf and the meter was shielded from direct sunlight.

Disease monitoring (bacterial canker of kiwifruit and tomato bacterial speck) was assessed at 21, 28, 35 and 42 days postinoculation (dpi) by measuring the following parameter:

- number of necrosis in each single leaf for each plant and calculation of the average number of necrosis per plant (*ANP*);
- number of symptomatic leaves related to the total leaves for each plant (*NSL*).

For each plant, a disease index (*DI*) was calculated with the equation $DI = ANP \times NSL$.

For each treatment, the average *DI* was obtained by averaging the *DI* from the single monitored plant.

The *DI* for olive knot was not assessed as symptoms need >90 days to be visible on plants.

Data for NBI and DI were obtained from three independent experiments organized as a complete randomized block, each one consisting of 10 plants for each experimental group.

2.4 Evaluation of resistance induction by quantitative real-time (qRT)-PCR

The relative expression level of the genes listed in Supporting Information, Tables S1–S3 was evaluated. Treated, inoculated and mock-treated leaves were harvested 48 h postinoculation (hpi) and immediately stored in liquid nitrogen and at −80 °C. Then, 100 mg fine powder was subjected to RNA extraction following the instructions provided by GRS Total RNA Kit-Plant (GRiSP Research Solutions, Porto, Portugal). The RNA was resuspended in Rnase-free sterile distilled water and immediately poured onto ice and quantified with Qubit™ RNA BR Assay Kit (Thermo Fisher Scientific). RNA integrity was checked by running 5 µL total RNA on 1.5% agarose gel. cDNA synthesis was performed using 500 ng RNA following the instructions provided by Xpert cDNA Synthesis Supermix with a gDNA eraser (GriSP Research Solutions) in a final volume of 20 µL. To check cDNA quality, a PCR was performed using cDNA as template to amplify *AcPP2A*, *SlACT* and *OeUBI* from samples derived from kiwifruit, tomato and olive, respectively. Tables S1–S3 show the list of target genes, accession numbers, their functions, the corresponding primer pairs, and their references used to perform the qRT-PCR. For the primer pairs designed in this study, sequence-similarity searches were carried out starting from known sequences obtained from Gramene (www.gramene.org, accessed on 18 October 2021). The sequences were submitted to BLASTN (https://blast.nlm.nih.gov/) analysis in order to extract the corresponding cDNA. Primers for qRT-PCR were designed inside the exonic regions by using PRIMER-BLAST (https://blast.ncbi.nlm.nih.gov/tools/primer-blast/). The optimal annealing temperature was assessed by running a gradient PCR for each primer pair.

Pest Management Science published by John Wiley & Sons Ltd on behalf of Society of Chemical Industry.

The relative expression levels of the target genes were calculated on the basis of the Cq values of the four technical replicates derived from three independent biological replicates for each plant species and treatment by applying the equation: *Relative expression* : $2^{-\Delta\Delta Cq}$, using *AcACT, AcPP2A, AcEF* or *OeTUB, OeUBI, OeACT* or *SlUBI, SlACT* as reference genes. Mock treatments were used to normalize the relative expression levels. The qRT-PCR was performed following the instructions provided by Rotor-Gene Q (Qiagen, Hilden, Germany) and Xpert Fast SYBR (uni) MasterMix (GriSP Research Solutions) in a final volume of 10 µL. The amplification conditions consisted of an initial denaturation step of 3 min at 95 °C; 40 cycles of 5 s of denaturation at 95 °C, 30 s of annealing at 55 °C for *AcPAL* and 60 °C for the remaining primer pairs for kiwifruit, olive and tomato, 20 s of elongation at 72 °C. A final melt cycle (70–99 °C) was performed to confirm the unicity of the amplicons and the absence of any gDNA contamination. NTC controls were included and the amplification was considered negative when a value of Cq ≥38 was detected.[28]

2.5 Quantification of bacterial spread inside the host tissues

For quantification of bacterial biomass by qRT-PCR, at 21, 28, 35 and 42 dpi, 10 random leaves from each independent replicate of each experimental group were homogenized. Then, 100 mg of every pathogen fresh culture and 100 mg plant material of each host leaves were subjected to total DNA extraction following the protocol for the GRS Genomic DNA Kit-Plants (GriSP research Solutions). DNA was quantified with a Qubit™ fluorometer 1.01 (Invitrogen) using the Qubit™ dsDNA BR Assay Kit (Thermo Fisher Scientific). DNA from inoculated samples was diluted to 10 ng μL^{-1}, whereas bacterial and plant calibration curves were obtained by preparing four serial 1:10 dilutions (1:1, 1:10, 1:100, 1:1000) from fresh bacterial cultures and uninoculated plant material DNAs. qRT-PCR was performed following the instructions from Rotor Gene Q (Qiagen) and Xpert Fast SYBR (uni) Master Mix (GriSP Research Solutions). The qRT-PCR amplification conditions included an initial denaturation step of 3 min at 95 °C; 40 cycle of 5 s of denaturation at 95 °C, 30 s of annealing at 60 °C for amplification of Psa and Psav target sequences or 50 °C for amplification of the Pst target sequence, 20 s of elongation at 72 °C. A final melt cycle (70–99 °C) was performed to confirm the amplicon's unicity. All of the primer pairs used are listed in Table S4. Data were obtained from four technical replicates derived from three biological replicates. Results were expressed as ng bacterial DNA per ng plant DNA.

2.6 Statistical analysis

Data were subjected to one-way analysis of variance (ANOVA). One level of significance ($P < 0.01$) was computed to assess the significance of the *F*-values. A pairwise analysis was carried out using the Tukey's honestly significant difference test (Tukey test) at the 0.99 confidence level. Statistical analyses were performed using DSAASTAT v1.022. Heatmaps were generated to represent the relative expression levels of kiwifruit, tomato and olive genes after the plant treatments (Tartu, Estonia).[29]

3 RESULTS

3.1 Individuation of the optimal CH and GA concentrations to assemble the NPF

Neither CNC nor HAS displayed antibacterial activities against Psa, Pst and Psav, demonstrating that their only function in the final NPF was that of carrier and excipient, respectively [Fig. S1(A)–(C)]. The employment of CH almost completely inhibited Psa and Psav proliferation at concentrations ranging from 0.01% to 1%, while only the highest concentrations (0.5% and 1%) completely inhibited Pst growth. GA displayed a strong antibacterial activity even at the lowest concentration and, in a similar way to CH application, Psa and Psav proliferation was more sensitive to GA at lowest concentrations than Pst proliferation. In general, GA ranging from 0.05% to 1% completely inhibited bacterial growth. For these reasons, we decided to employ CH at 0.5% and GA at 0.05% to assemble the NPF. The synergistic antibacterial activity of CH + GA was comparable to the activity of the single molecules when applied against Psa and Psav [Fig. S2(A)–(C)]. However, the CH and GA mixture demonstrated antibacterial properties against Pst as great as GA and higher than CH alone, suggesting that the predominant antibacterial properties are displayed by GA.

3.2 The NPF demonstrated direct antimicrobial activity and mechanical interaction with bacterial cells

The broth assay demonstrated that the NPF did not influence Psa biomass accumulation and biofilm synthesis in liquid medium. Pst biomass formation was not affected by the NPF compared to mock control, while $Cu(OH)_2$ reduced Pst cell multiplication in liquid broth. The NPF favoured biofilm synthesis in Pst compared to the mock control (average recorded absorbance 0.46 and 0.24 in NPF and mock samples, respectively). The NPF did not affect Psav biomass formation compared to mock control, whereas $Cu(OH)_2$ inhibited cells multiplication. The NPF favoured biofilm synthesis in liquid broth compared to the mock control (average recorded absorbance was of 0.62 and 0.28 in NPF and mock samples, respectively) [Fig. 1(A)–(C)].

The incorporated assay demonstrated that the NPF had antimicrobial properties by direct contact with all the three *Pseudomonas* spp. The average radial growth of Psa colonies was 9.08 mm in the NPF samples and 25.83 mm in the mock samples. The average radial growth of Pst colonies was 9.58 mm in the NPF samples and 21.67 mm in the mock samples. The average radial growth of Psav colonies was 10.42 mm in the NPF samples and 30.50 mm in the mock samples The incorporation of $Cu(OH)_2$ into the medium completely inhibited the colonies' radial growth [Fig. 1(D)–(G)].

The NPF mechanically interacted with bacterial cells. The application of NPF increased Psa bacterial cells aggregation at 0 and 24 hpi compared to $Cu(OH)_2$ and mock, and also at 48 hpi compared to mock samples. At 48 hpi, the average recorded absorbance was of 0.17 in the NPF samples, 0.08 in the $Cu(OH)_2$ sample and 0.00 in the mock controls. The NPF increased Pst bacterial cells aggregation at 0, 24 and 48 hpi compared to mock controls. At 48 hpi, the average recorded absorbance was of 0.19 in the NPF samples, 0.2 in the $Cu(OH)_2$ samples and 0.00 in the mock controls. The NPF favoured Psav bacterial flocculation during all time points. At 72 hpi, the average recorded absorbance was of 0.18 in the NPF samples, −0.02 in the $Cu(OH)_2$ samples and 0.00 in the mock samples [Fig. 2(A)–(C)]. Figure 2(D)–(F) shows that the NPF did not influence bacterial cells adhesion compared to mock controls, while $Cu(OH)_2$ decreased bacterial cells adhesion for all the three *Pseudomonas* spp.

3.3 The NPF displayed biocompatibility on kiwifruit, tomato and olive plants, while counteracting the symptomatic progression of kiwifruit bacterial canker and tomato bacterial speck

Treatments with $Cu(OH)_2$ resulted in lower NBI values compared to the mock control in kiwifruit and tomato plants, whereas no significant differences were recorded in the NPF-treated leaves

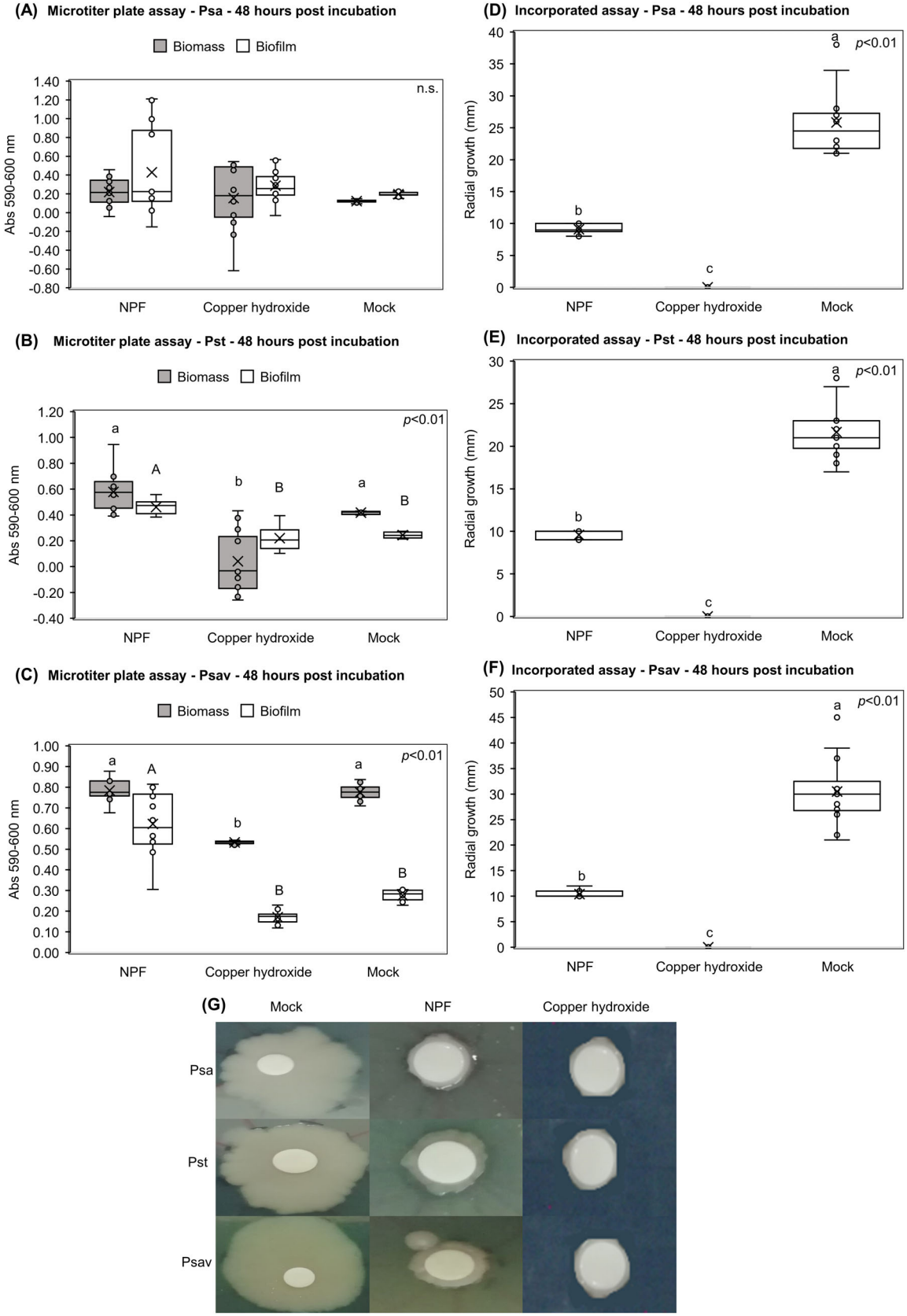

Figure 1. Boxplots of the in-broth microtitre well assay against *Pseudomonas syringae* pv. *actinidiae* (Psa) (A), *P. syringae* pv. *tomato* (Pst) (B) and *P. savastanoi* pv. *savastanoi* (Psav) (C) bacterial cells. Boxplots of the incorporated assay against Psa (D), Pst (E) and Psav (F). Pictures of bacterial colonies grown on King's B (KB) or KB incorporated with the NPF or $Cu(OH)_2$ at 48 h post incubation (G). Different letters (a, A, b, B, c, C) in the subfigures refer to the statistical analysis performed using one-way analysis of variance (ANOVA) with the Tukey test at a confidence level of 0.99 and $P < 0.01$, while 'n.s.' stands for 'not significant'. Lowercase and uppercase letters (in A, B, C) refer to two different ANOVA and Tukey tests.

Pest Management Science published by John Wiley & Sons Ltd on behalf of Society of Chemical Industry.

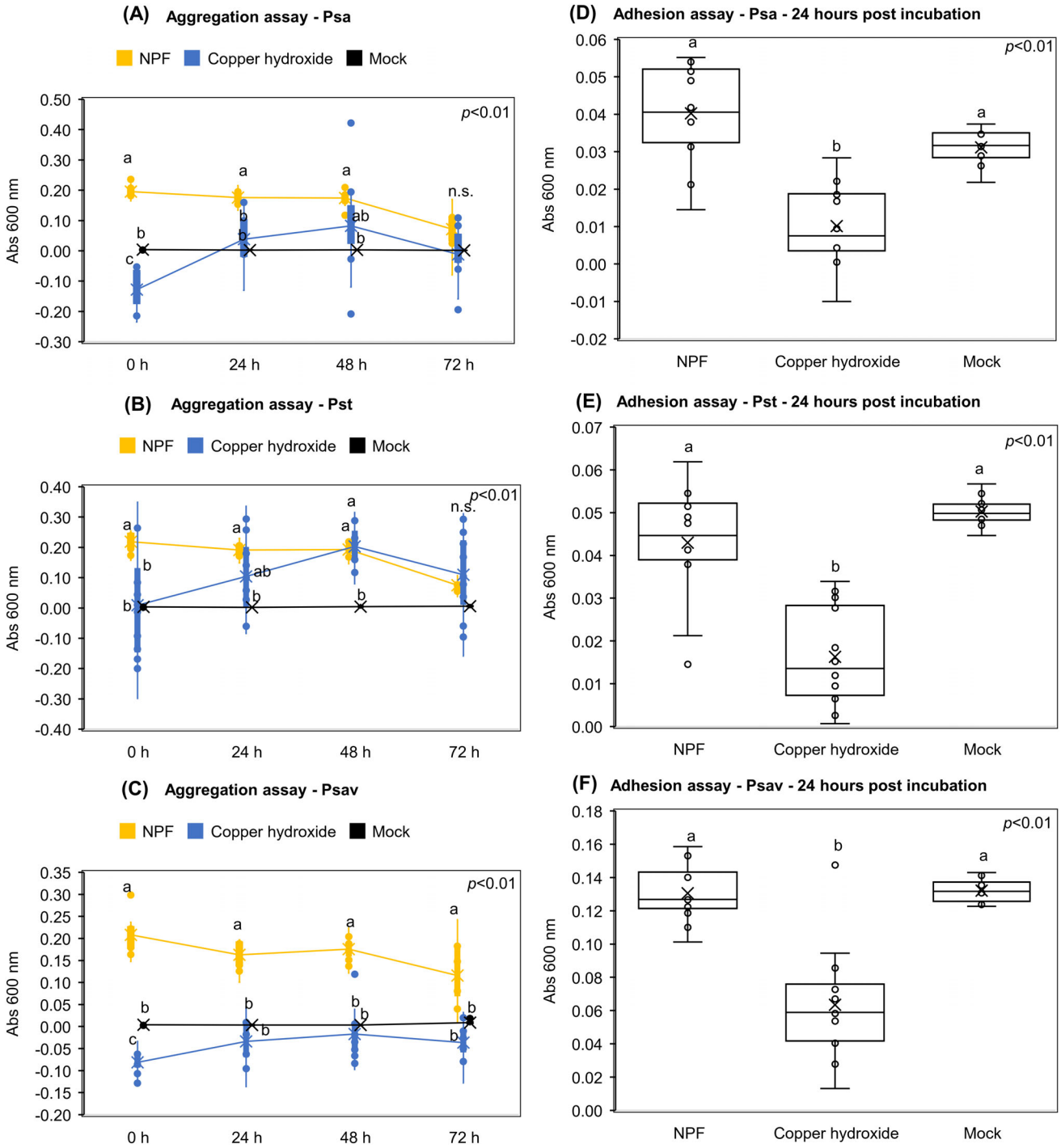

Figure 2. Boxplots of the aggregation assay against *Pseudomonas syringae* pv. *actinidiae* (Psa) (A), *P. syringae* pv. *tomato* (Pst) (B) and *P. savastanoi* pv. *savastanoi* (Psav) (C) bacterial cells. Boxplots of the adhesion assay against Psa (D), Pst (E) and Psav (F) bacterial cells. Different letters (a, b, c) into the subfigures refer to the statistical analysis performed using one-way analysis of variance (ANOVA) with the Tukey test at a confidence level of 0.99 and $P < 0.01$, while 'n.s.' stands for 'not significant'.

compared to both $Cu(OH)_2$- and mock-treated plants. Average NBI values were 28.59, 15.26 and 40.38 in the NPF-, $Cu(OH)_2$- and mock-treated kiwifruit plants, and 73.92, 67.61 and 86.78 in the NPF-, $Cu(OH)_2$- and mock-treated tomato plants. No statistical differences were recorded in treated olive plants between the three treatments [Fig. 3(A)–(C)].

The application of NPF on kiwifruit plants decreased the symptomatic progression from 28 to 42 dpi. The DI in the NPF-treated plants was lower than in the $Cu(OH)_2$-treated or solely inoculated plants. At 42 dpi the average DI was 0.89, 6.09 and 7.26 in the NPF-, $Cu(OH)_2$- and mock-treated kiwifruit plants. The NPF application was more effective than $Cu(OH)_2$ in reducing the kiwifruit bacterial canker symptom progression. In tomato plants, the NPF application decreased the symptomatic progression at 35 and 42 dpi as much as $Cu(OH)_2$. At 42 dpi the average DI was 1.92, 2.02 and 2.34 in the NPF-, $Cu(OH)_2$- and mock-treated tomato plants [Fig. 4(A)–(C)].

3.3.1 *The NPF activated the systemic acquired resistance (SAR)-related pathways in kiwifruit and olive plants*

The expression of the main genes involved in the induction of SAR was evaluated under artificial inoculation and treatments conditions. Figure S3 shows that the synthetized cDNA from RNA extracted from kiwifruit, tomato and olive leaves was successfully amplifiable. Figure S4 shows that all the selected pair of primers selectively amplified the target sequences. Figure 5 represents the heatmaps obtained by calculating the *z*-score, while the relative expression level of each analyzed gene is shown into the corresponding heatmap. In kiwifruit plants, the NPF slightly upregulated *AcCHI* (1.65-fold), *AcPR1* (1.82-fold), *AcWRKY* (1.87-fold) and *AcPR5* (1.74-fold). The application of NPF increased the expression level of *AcCHI*, *AcPR1*, *AcWRKY* and *AcPR5* compared to Psa inoculation and $Cu(OH)_2$ treatment. *AcLOX* was slightly upregulated by Psa artificial inoculation (1.19-fold) compared to NPF (1.01-fold) and $Cu(OH)_2$ (0.96-fold) treatments, whereas the expression of *AcPAL* (2.14-fold) increased after the $Cu(OH)_2$ treatment. In tomato plants, only *SlCHI* was upregulated by the NPF treatment (1.85-fold) as much as Pst artificial inoculation (2.32-fold). Pst inoculation boosted the expression levels of *SlCHI* and *SlWRKY* (4.75-fold), whereas $Cu(OH)_2$ drastically increased the expression of *SlPR1* (12.00-fold). The application of the NPF on olive plants strongly boosted all of the analyzed genes. The NPF upregulated *OeCHI* (69.33-fold) as much as Psav inoculation (86.98-fold), yet was only slightly upregulated in $Cu(OH)_2$-treated plants (8.42-fold); the NPF treatment also boosted the expression of *OeLOX* (38.86-fold), *OeWRKY* (11.32-fold), *OePR5* (90.36-fold), *OePR2* (49.98-fold), *OePAL* (21.03-fold) and *OeNPR1* (26.98-fold) compared to Psav inoculation and $Cu(OH)_2$ treatment [Fig. 5(A)–(C)].

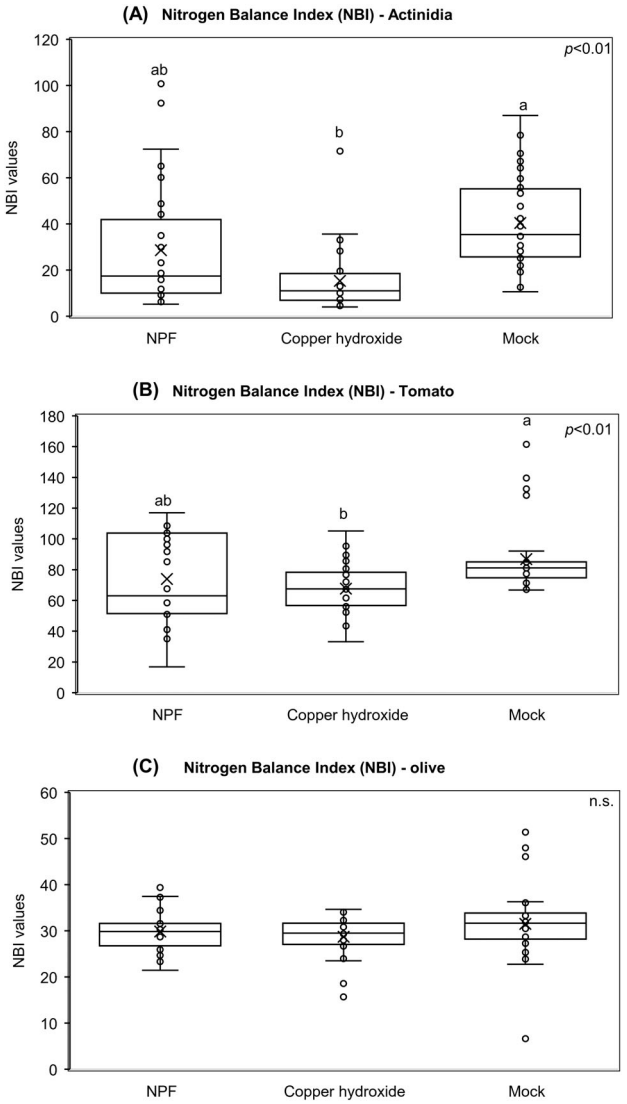

Figure 3. *In planta* biocompatibility assay. Boxplots of the NBI measurements in kiwifruit (A), tomato (B) and olive (C) plants. Different letters (a, b) in the subfigures refer to the statistical analysis performed using one-way analysis of variance (ANOVA) with the Tukey test at a confidence level of 0.99 and $P < 0.01$, while 'n.s.' stands for 'not significant'.

3.4 Application of NPF inhibited bacterial spread on plants

Figure S5 represents the target sequences from pure Psa, Pst and Psav gDNA to test the primer pairs efficiency and specificity. Figure 6 shows the amplification and the calibration curves obtained from total gDNA of kiwifruit, tomato, olive, Psa, Pst and Psav. The R^2 coefficient ranged from 0.935 to 0.997 demonstrating the accuracy among replicates and dilutions employed to obtained the calibration curves. Figure S6 shows the melting curves of the amplification products from samples used to obtain the calibration curves, demonstrating the amplicon unicity and specificity of the primer pairs used to detect Psa, Pst and Psav. No significant differences were observed among the different treatments at 21, 28 and 35 dpi in the reduction of Pst and Psav biomass spread, and at 21 and 35 dpi in the reduction of Psa spread. At 28 dpi, the application of NPF mitigated Psa spread as much as the application of $Cu(OH)_2$ (Table S5). However, promising data were collected at 42 dpi: the application of NPF reduced Psa, Pst and Psav bacterial spread. The preventive application of NPF reduced Psa spread more efficiently that $Cu(OH)_2$ (13.80 and 54.70 ng ng^{-1}, respectively). The application of NPF in tomato plants was effective as much as $Cu(OH)_2$ in reducing the amount of Pst DNA accumulation (1.42 and 1.72 ng ng^{-1}, respectively); the preventive NPF treatment reduced the accumulated Psav DNA (3.23 ng ng^{-1}), whereas $Cu(OH)_2$ was ineffective compared to the solely inoculated plants (3.91 and 4.08 ng ng^{-1}, respectively) [Fig. 7(A)–(C)].

4 DISCUSSION

We evaluated the putative antimicrobial and elicitor-like properties of a third generation, nanotechnology-based agrochemical, NPF, composed of CNC as carrier, HAS as excipient, CH and GA as active molecules. This NPF had already been tested as fungicide against *F. graminearum* and *F. culmorum*, boosting innate immunity in three bread wheat genotypes.[22] The NPF inhibited *in vitro* conidia germination and mycelium growth, while reducing their adhesion. On plants, the NPF reduced Fusarium head blight (FHB) and Fusarium crown rot (FCR) in three bread wheat genotypes. Application of the NPF on plants boosted several genes involved in SAR activation. The application of the NPF was biocompatible and reduced the accumulated fungal biomass into the flours. Starting from these lines of evidence, we decided to investigate the applicability the NPF in counteracting three impacting bacterial plant pathogens, Psa, Pst and Psav, as much as its potentialities as beneficial treatment for plant health status and innate immunity.

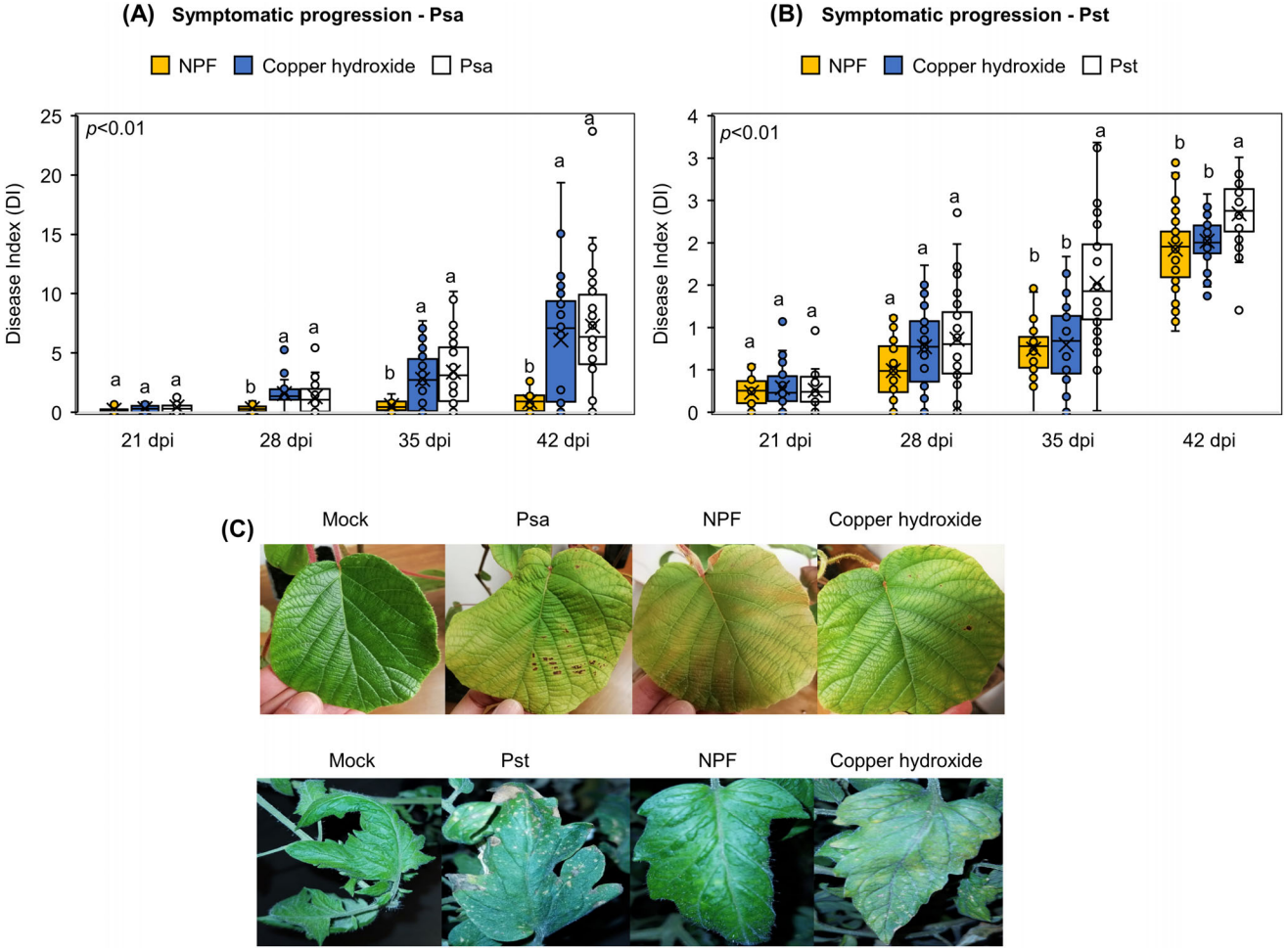

Figure 4. *In planta* symptomatic progression. Severity of bacterial canker of kiwifruit (A) and of bacterial speck of tomato (B). Different letters (a, b) in the subfigures refer to the statistical analysis performed using one-way analysis of variance (ANOVA) with the Tukey test at a confidence level of 0.99 and $P < 0.01$. Representative pictures of treated and inoculated kiwifruit and tomato leaves at 42 dpi (C).

CNC and starch have been investigated as carriers and excipient, respectively, to vehicle active molecules, and to enhance their chemical properties, stability and solubility in agrochemicals. CNC have been used to deliver carvacrol to control three bacterial plant pathogens,[30] which contrasted *in vitro* bacterial multiplication. CNC and starch also have been added as surfactants to poly(DL-lactide-co-glycolide) nanoparticles and demonstrated to counteract Pst survival on tomato plants.[31] A very similar composite to the NPF was investigated against Pst. The composite was made of CNC, starch and CH. Conventional starch and HAS were compared to investigate their different abilities in CH loading capacity and release, and resulted completely equivalent for their putative usage as excipient.[32]

CH and GA have been functionalized to CNC and HAS as active antimicrobials. The antimicrobial properties of CH have been widely reviewed and investigated.[33–36] The *in vitro* antibacterial activity of CH against Psa was demonstrated by incorporated assay into agar medium[37] and its antimicrobial activity also has been validated in field experiments. CH reduced Psa symptoms more efficiently than $Cu(OH)_2$, while reducing the presence of exudates on the trunk. Moreover, CH did not show any phytotoxicity on plants and fruits.[38] CH extracted from shrimp exoskeletons demonstrated *in vitro* antibacterial properties against Pst. The same study demonstrated also that CH significantly reduced the disease incidence in pretreated seedlings.[39] A nanotechnology-based agrochemical composed of CNC, starch and CH was employed at 1% and inhibited Pst growth both *in vitro* and *in vivo* as much as $Cu(OH)_2$ used as reference agrochemical. At the same time, the composite demonstrated full biocompatibility on tomato plants.[33] To the best of our knowledge, CH bulk materials or CH-based nanoparticles have never been investigated to control Psav, and thus the present research represents the first evidence that CH could be successfully employed against the bacterial olive knot disease. GA also had already been investigated for the mitigation of the kiwifruit bacterial canker. GA inhibited *in vitro* Psa by the paper disc diffusion test. GA was encapsulated in methacrylate polymeric microparticles and tested *in vivo* and in field trials. The encapsulation improved the GA antibacterial properties and lasted remarkably for ≤14 days after the treatments.[40] GA and GA-enriched extracts also were tested against Pst. The employment of GA-based tannins allowed the reduction of cupric salts to manage tomato bacterial speck. This powerful effect was confirmed during *in planta* experiments, where GA-based tannins applied alone and mixed with the half field dose of $Cu(OH)_2$ were as effective in preventing symptom occurrence as the recommended field dose of $Cu(OH)_2$. GA-based

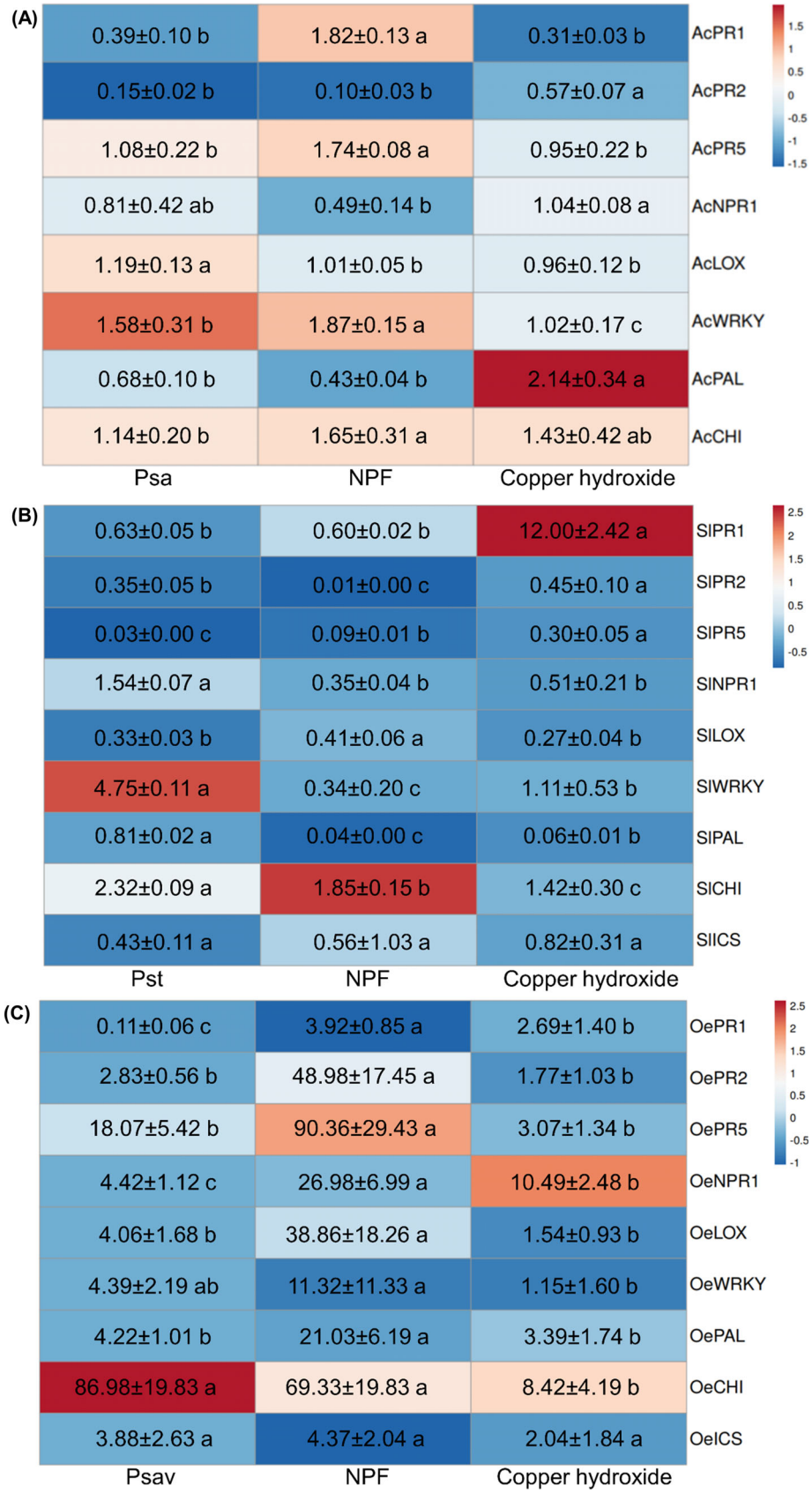

Figure 5. Heatmaps, relative expression levels, and standard deviations of the selected kiwifruit (A), tomato (B) and olive (C) genes in the NPF-treated, $Cu(OH)_2$-treated and solely inoculated plants. The heatmaps were constructed with the *z*-score (explained by the colour legend at the left of the picture) by analyzing data with ClustVis software (Tartu, Estonia).

Pest Management Science published by John Wiley & Sons Ltd on behalf of Society of Chemical Industry.

formulations did not show any detrimental properties on tomato plants, because their application boosted NBI values as much as the plant dry biomass.[41] Another study evaluated the effect of *Punica granatum* fruit peel extract, rich in GA, and its employment reduced Pst colonies growth both *in vitro* and *in vivo*. The authors observed that the effect of the extract-based treatments lasted up

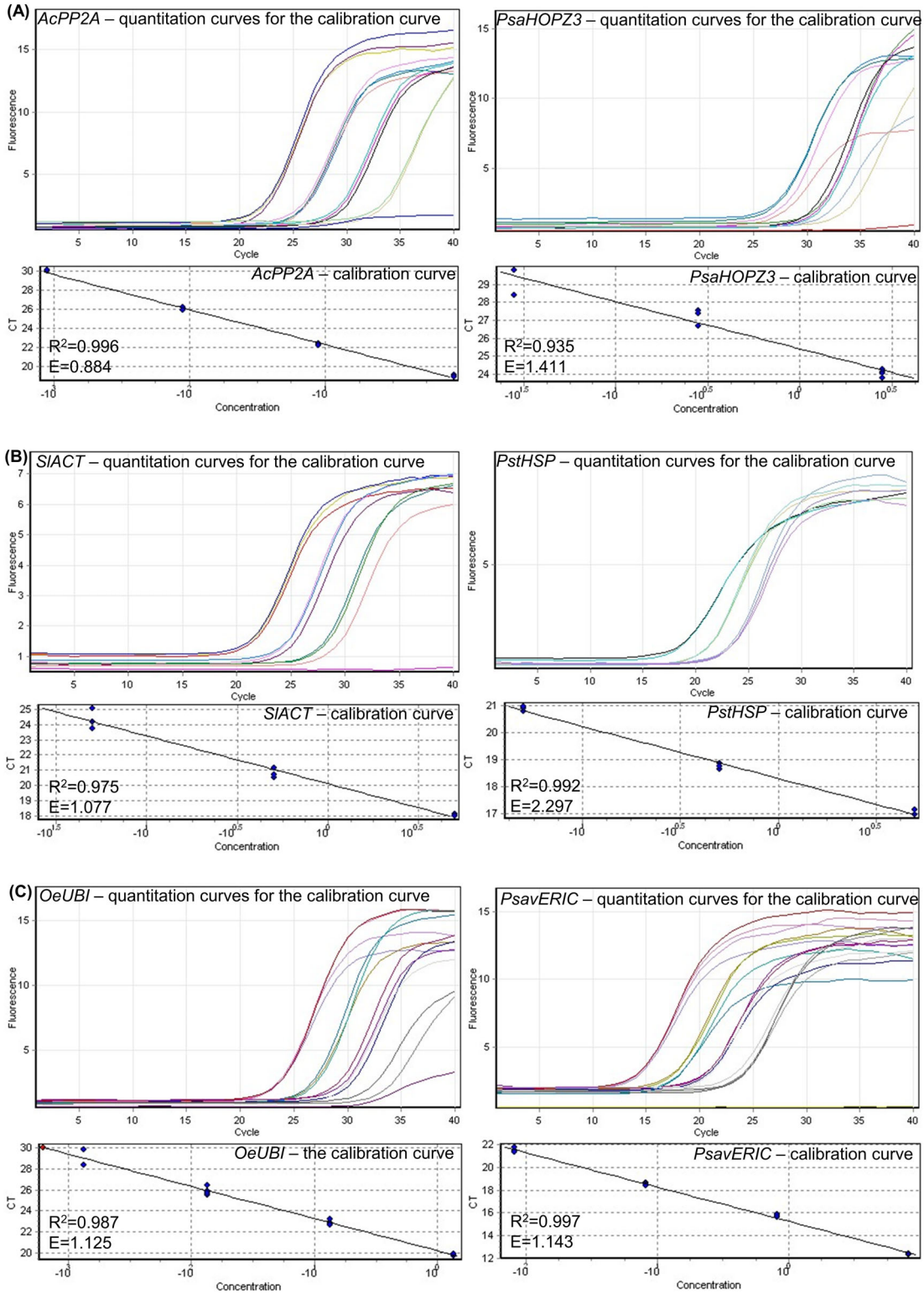

Figure 6. Calibration curves set up for DNA quantification. Quantitation and calibration curves for *AcPP2A* and *PsaHOPZ3* (A), *SlACT* and *PstHSP* (B), *OeUBI* and *PsavERIC* (C).

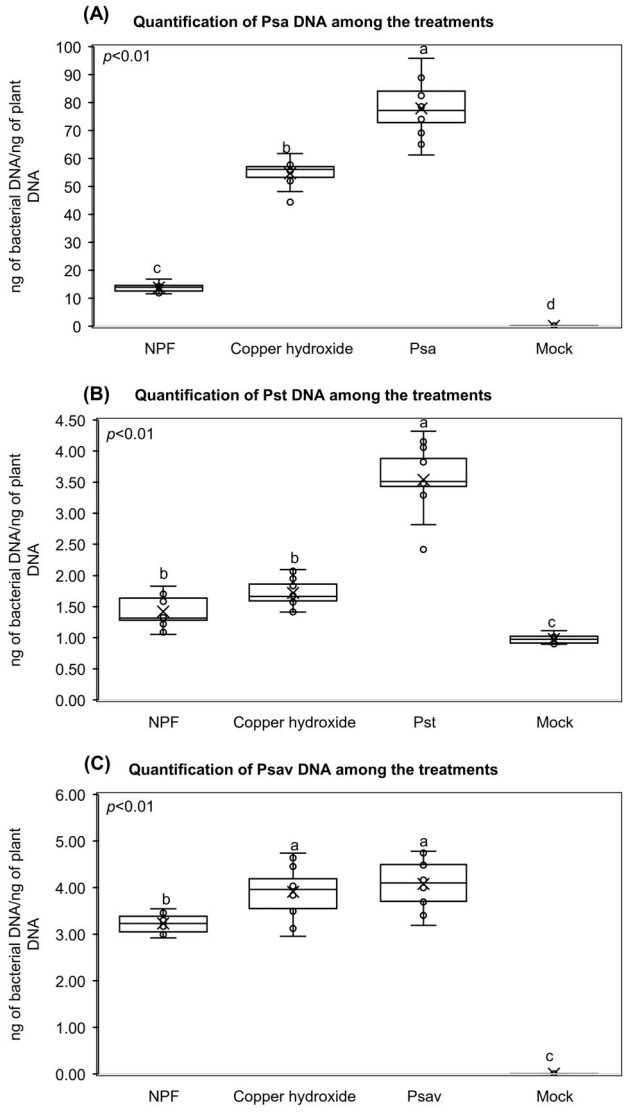

Figure 7. *Pseudomonas syringae* pv. *actinidiae* (Psa) (A), *P. syringae* pv. *tomato* (Pst) (B) and *P. savastanoi* pv. *savastanoi* (Psav) (C) biomass quantification at 42 dpi expressed as ng bacterial DNA per ng plant DNA. Different letters (a, b, c, d) in the subfigures refer to the statistical analysis performed using one-way analysis of variance (ANOVA) with the Tukey test at a confidence level of 0.99 and $P < 0.01$.

to 15 days, which is considered longer than that after application of conventional cupric-based salts.[42] A GA-rich extract from dried leaves of *Eucalyptus globulus* was tested against Pst and demonstrated to completely inhibit the pathogen *in vitro* and *in vivo*, because it suppressed the hypersensitive response when the bacterial suspension was infiltrated onto tobacco leaves. The authors highlighted that the GA-based extract impaired cell viability by >86%.[43] GA-based microparticles also have been prepared using hydroxyl-propyl-methylcellulose-phtalate and ethyl cellulose and tested *in vivo* against Pst. The treatment significantly reduced Pst epiphytic population with comparable activity to copper salts.[44] GA-based extracts also were tested against Psav. A GA-containing extract obtained from olive mill wastewaters displayed *in vitro* antimicrobial activity against Psav.[45] Another research study demonstrated that the GA-based extract from *Lawsonia inermis* inhibited *in vitro* Psav growth as much as the formation of knots on twigs of olive plants.[46] Taken together, this evidence regarding the antibacterial properties of CH and GA are in line with those observed in the present research work, because the NPF inhibited Psa, Pst and Psav by agar *in vitro* assay, but not in liquid broth, probably because the NPF was not completely bioavailable in liquid compared to agar medium. At the same time, we also observed a mitigation in symptom spread for the kiwifruit bacterial canker and bacterial speck of tomato, confirming the data already present in literature.

We also evaluated the putative mechanical interaction of the NPF with bacterial cells by monitoring biofilm biosynthesis, cellular aggregation and cellular adhesion. We observed that treating bacterial cells with the NPF into KB broth medium does not affect biofilm biosynthesis (Psa) or even increase its production (Pst, Psav), while favouring bacterial cell aggregation and adhesion. Biofilm is defined as cooperating communities of surface-associated bacteria enclosed in extracellular polymeric substances (EPS) composed of proteins, polysaccharides and DNA. Biofilm is responsible for various functions, such as modulation of metabolism, response to nutrient uptake, cell-to-cell communication and contact, in addition to restricting the access of antimicrobial agents. Many research papers and reviews already reported that biofilm-growing cells express distinct characteristics from planktonic ones, such as an increased resistance to antimicrobial compounds. This could be related to the physical and/or chemical structures of EPS that could confer resistance by exclusion of biocides molecules from the bacterial community, thus resulting in the development of a biofilm-specific antimicrobial-resistant phenotype.[47–49] This may explain why no antimicrobial activity was observed in the NPF- and $Cu(OH)_2$-treated biofilm-aggregated bacterial cells, with no effect or even an increase in biofilm production. Biofilm also is involved in cell-to-cell aggregation and adhesion to the surface, because it represents an adaptive strategy for successful host colonization.[47,50] As a result, we also observed an increase in cellular aggregation and adhesion, which can be explained by the increase of biofilm biosynthesis in benthic cells.

The expression of some SAR-related genes revealed that Psa inoculation slightly upregulated three genes (*AcCHI*, *AcLOX*, *AcWRKY*), NPF upregulated four genes (*AcCHI*, *AcPR1*, *AcWRKY*, *AcPR5*), and $Cu(OH)_2$ upregulated two genes (*AcCHI* and *AcPAL*) in kiwifruit leaves. Several other research papers and reviews have highlighted that the activation of SAR is linked to resistance against Psa.[51,52] The activation of pathogenesis-related proteins seems to play a key role for the mitigation of the bacterial canker of kiwifruit.[53] Kiwifruit plants treated with chitosan displayed upregulation of *AcPR1* and *AcPR5* at 24 and 48 hpi, demonstrating a symptom reduction in inoculated plants.[54] Despite the lack of research studies investigating the expression level of *AcCHI* in response to Psa or elicitor-like molecules, a few proteomics and metabolomics investigations revealed that the biosynthesis of chitinase is boosted during the early stage of Psa infection, which could be an indirect proof of high *AcCHI* transcript levels.[55,56] Plant chitinases are a group of enzymes that hydrolyze chitin from insects, fungi or bacteria and are involved in defence mechanisms against biotic attacks. Because NPF also is composed of CH, this could act as a plant elicitor of chitinases, especially because the *AcCHI* relative expression in the NPF-treated leaves was higher than in the Psa-infected plants. WRKY are a class of transcription factors playing a critical role in plant defence response against both abiotic and biotic stresses. We observed an upregulation of *AcWRKY* in the NPF-treated leaves, compared to Psa inoculated

and $Cu(OH)_2$-treated leaves. It is already reported that the activation of *AcWRKY* is related to Psa resistance in kiwifruit, so we can conclude that the NPF acts as an elicitor of *AcWRKY* transcription factors.[53,57,58] PAL catalyses the transformation of L-phenylalanine to *trans*-cinnamate, which is the first step for biosynthesis of phenylpropanoids, having many metabolic roles in response to light stimuli, plant defence, growth regulation and differentiation.[59] We observed an upregulation of *AcPAL* in the $Cu(OH)_2$-treated kiwifruit leaves. Some works have already observed that cupric salts may contribute in the enhancement of PAL activity, and the induction of defences after treating plants with cupric salts was observed in grapevine, which is closely related to kiwifruit.[60,61] This evidence may explain the upregulation of *AcPAL* in $Cu(OH)_2$-treated plants. The discussed works taken together are in line with the data observed in the present work, where we can affirm that the NPF can act as an elicitor in kiwifruit plants, thus contributing to the reduction of kiwifruit bacterial canker symptoms.

A completely different behaviour was observed in tomato plants, where Pst artificial inoculation upregulated *SlCHI*, *SlWRKY* and *SlNPR1*, NPF boosted the transcripts of *SlCHI*, and $Cu(OH)_2$ greatly upregulated *SlPR1*, suggesting that the application of the NPF in tomato leaves does not act as an elicitor as much as in kiwifruit plants. This is in contrast with previous observations, where CH oligosaccharide boosted both the salicylic acid and jasmonic acid pathways in *Arabidospis* plants.[62] This could be explained by the fact that *S. lycopersicum* can react differently than *Arabidospis* or the presence of CNC, HA starch and GA can mask CH elicitor-like properties. In particular, antifungal activity and activation of defence responses to oxidative stress after application of GA in tomato have been already studied,[63,64] but no research is available regarding the GA elicitor-like behaviour in tomato. At the same time, the application of CNC or HA starch to boost innate immunity in tomato has never been investigated. For these reasons, we can speculate that the presence of CNC, HA starch or GA can mask the elicitor-like activity displayed by CH. This also is reflected in the tomato bacterial speck symptom progression after the preventive application of NPF, because the symptom reduction observed in tomato was not so considerable as in kiwifruit plants. This could mean that the slower Pst symptom reduction is mainly due to the direct NPF antibacterial activity.

In olive plants, a remarkable upregulation of all of the selected genes was observed in the NPF-treated plants, with a special reference to the transcript levels of *OeCHI*, *OeLOX*, *OePR5* and *OePR2*, followed by *OePAL*, *OeNPR1* and *OeWRKY*. Despite that the application of CH and polysaccharide-based extracts had already demonstrated the activation of PAL and the accumulation of polyphenols in olive plants,[65,66] no studies have been carried out regarding the evaluation of the expression genes related to the induction of SAR in olive plants. For this reason, it is quite hard to compare our data with the literature, and we can affirm that this is the first paper reporting that a composite of CH, GA, CNC and HA starch acts as a strong elicitor in olive plants. Moreover, to the best of our knowledge, the induction of defences in olive plant in response to Psav infection have been poorly investigated. Indeed, nothing has been found in the literature regarding the role of genes involved in biosynthesis of salicylic acid or induction of SAR in response to Psav infection in olive plants. Thus, we can affirm that this is the first research to individuate at least nine key responsive genes to Psav infection, all related with the induction of SAR in olive plants.

Bacterial spread after a treatment is often evaluated by counting recorded colonies, which is labour-intense, time-consuming, and with no high-throughput and specific quantification method being validated. For these reasons, we decided to evaluate Psa, Pst and Psav spread by molecular tools, to be specific, selective, reliable and fast during data collection. Many papers report several molecular based assays for the quantification of Psa, Pst and Psav,[67–72] but no research studies regarding the bacterial pathogen quantification in response to an antibacterial treatment are already present in literature. We employed already published primer pairs, specifically designed to detect and quantify Psa, Pst and Psav, and reference genes specifically designed to detect and quantify kiwifruit, tomato and olive plant DNA, in order to relate the bacterial DNA amount to the plant DNA amount. Thus, we were able to quantify the accumulated bacterial biomass after the NPF treatment. To the best of our knowledge, this represents the first research paper reporting this molecular based-approach to monitor bacterial spread in relationship to a mitigation strategy. The quantification of bacterial spread revealed that bacterial accumulation resulting from the NPF treatment was affected only at 42 dpi, whereas symptom scoring revealed that DI was lower at 28, 35 and 42 dpi in tomato plants, and at 35 and 42 dpi in kiwifruit plants. This could be explained by the fact that, as observed by *in vitro* experiments, the NPF does not negatively affect biofilm synthesis and adhesion capability of bacterial cells, but instead showed direct antibacterial activity during agar assay, and boosted innate immunity in kiwifruit and olive plants. Thus, we can hypothesize that sprayed bacterial cells on leaves after the NPF treatment still continue to multiply but their virulence could be somehow reduced. This means that the synergistic activity between direct antibacterial activity and elicitor-like properties could contribute to reduce symptoms development on leaves and accumulation of bacterial spread at the late stages of infection. Starting from these results, we can affirm that further experiments are need to elucidate if the NPF can prolong its elicitor-like properties by extending the time between treatment and inoculation.

5 CONCLUSIONS

We demonstrated that a third generation, nanotechnology-based and natural-derived antimicrobial composite, named as NPF, showed direct antibacterial activity against Psa, Pst and Psav, and boosted innate immunity in kiwifruit and olive plants. The NPF can be potentially synthetized starting from plant-derived wastes, as cellulose, starch and GA can be easily extracted from plant wastes, and CH is a food-derived waste. This means that the synthesis and employment of NPF completely matches with the upcoming requests from the European Green Deal, because it contributes both to synthetic pesticide reduction and enhances circular economy in agriculture. Based on our actual data, the NPF will be particularly promising for the mitigation of kiwifruit bacterial canker and bacterial olive knot, because it acts as a multi-site agrochemical and is especially for its interesting capabilities to boost the major genes involved in the activation of SAR. For this reason, the NPF could act as a valuable substitute to cupric-based salts, especially regarding the problematics related to selection of resistant pathogen strains.

ACKNOWLEDGEMENTS

The research was funded by Strategical Projects-Lazio Region Ads Green Economy D. D. no. G04052 GRAEEN Project; Italian Ministry for University and research (MUR) PON "Research and Innovation

2014-2020 of the National Smart Specialization Strategy (SNSI) and the National Research Plan (PNR). The Research was carried out in the framework of the National program for 'Departments of Excellence 2023-2027' of MUR (DiVerSo Project) at DAFNE, University of Tuscia.

CONFLICT OF INTEREST

The authors declare that the research was conducted without conflict of interest.

DATA AVAILABILITY STATEMENT

The data that supports the findings of this study are available in the supplementary material of this article

SUPPORTING INFORMATION

Supporting information may be found in the online version of this article.

REFERENCES

1 Donati I, Cellini A, Sangiorgio D, Vanneste JL, Scortichini M, Balestra GM *et al.*, *Pseudomonas syringae* pv. *Actinidiae*: ecology, infection dynamics and disease epidemiology. *Microb Ecol* **80**:81–102 (2020).
2 Vanneste JL, Emerging threats to the kiwifruit industry: *pseudomonas syringae* pv. *Actinidiae* (Psa): a threat to the New Zealand and global kiwifruit industry. *New Zeal J Crop Hortic Sci* **40**:265–267 (2012).
3 Vanneste JL, The scientific, economic, and social impacts of the New Zealand outbreak of bacterial canker of kiwifruit (*pseudomonas syringae* pv. *Actinidiae*). *Annu Rev Phytopathol* **55**:377–399 (2017).
4 Panno S, Davino S, Caruso AG, Bertacca S, Crnogorac A, Mandić A *et al.*, A review of the most common and economically important diseases that undermine the cultivation of tomato crop in the mediterranean basin. *Agronomy* **11**:2188 (2021).
5 Griffin K, Gambley C, Brown P and Li Y, Copper-tolerance in *pseudomonas syringae* pv. *Tomato* and *Xanthomonas* spp. and the control of diseases associated with these pathogens in tomato and pepper. A systematic literature review. *Crop Prot* **96**:144–150 (2017).
6 Lamichhane JR and Varvaro L, Epiphytic *pseudomonas savastanoi* pv. *Savastanoi* can infect and cause olive knot disease on *Olea europaea* subsp. *cuspidata*. *Australas Plant Pathol* **42**:219–225 (2013).
7 Buonaurio R, Moretti C, Da Silva DP, Cortese C, Ramos C and Venturi V, The olive knot disease as a model to study the role of interspecies bacterial communities in plant disease. *Front Plant Sci* **6**:434 (2015).
8 Turco S, Drais MI, Rossini L, Chaboteaux E, Rahi YJ, Balestra GM *et al.*, Complete genome assembly of the Levan-positive strain PVFi1 of *pseudomonas savastanoi* pv. *Savastanoi* isolated from olive knots in Central Italy. *Environ Microbiol Rep* **14**:274–285 (2022).
9 Lamichhane JR, Osdaghi E, Behlau F, Köhl J, Jones JB and Aubertot JN, Thirteen decades of antimicrobial copper compounds applied in agriculture. A review. *Agron Sustain Dev* **38**:1–18 (2018).
10 La Torre A, Iovino V and Caradonia F, Copper in plant protection: current situation and prospects. *Phytopathol Mediterr* **57**:201–236 (2018).
11 Hu HW, Wang JT, Li J, Li JJ, Ma YB, Chen D *et al.*, Field-based evidence for copper contamination induced changes of antibiotic resistance in agricultural soils. *Environ Microbiol* **18**:3896–3909 (2016).
12 Fagnano M, Agrelli D, Pascale A, Adamo P, Fiorentino N, Rocco C *et al.*, Copper accumulation in agricultural soils: risks for the food chain and soil microbial populations. *Sci Total Environ* **734**:139434 (2020).
13 Zhang X, Fu G, Xing S, Fu W, Liu X, Wu H *et al.*, Structure and diversity of fungal communities in long-term copper-contaminated agricultural soil. *Sci Total Environ* **806**:151302 (2022).
14 Chaka KT, Extraction of cellulose nanocrystals from agricultural by-products: a review. *Green Chem Lett Rev* **15**:582–597 (2022).
15 An C, Sun C, Li N, Huang B, Jiang J, Shen Y *et al.*, Nanomaterials and nanotechnology for the delivery of agrochemicals: strategies towards sustainable agriculture. *J Nanobiotechnol* **20**:1–19 (2022).
16 Rostamabadi H, Falsafi SR and Jafari SM, Starch-based nanocarriers as cutting-edge natural cargos for nutraceutical delivery. *Trends Food Sci Technol* **88**:397–415 (2019).
17 Cui C, Ji N, Wang Y, Xiong L and Sun Q, Bioactive and intelligent starch-based films: a review. *Trends Food Sci Technol* **116**:854–869 (2021).
18 Hou X, Wang H, Shi Y and Yue Z, Recent advances of antibacterial starch-based materials. *Carbohydr Polym* **302**:120392 (2023).
19 Hong Y, Liu G and Gu Z, Recent advances of starch-based excipients used in extended-release tablets: a review. *Drug Deliv* **23**:12–20 (2016).
20 Reglinski T, Wurms K, Vanneste J, Ah Chee A, Yu J, Oldham J *et al.*, Transient changes in defence gene expression and phytohormone content induced by acibenzolar-S-methyl in glasshouse and orchard grown kiwifruit. *Front Agron* **3**:831172 (2022).
21 Goupil P, Benouaret R and Richard C, Ethyl gallate displays elicitor activities in tobacco plants. *J Agric Food Chem* **65**:9006–9012 (2017).
22 Francesconi S, Ronchetti R, Camaioni E, Giovagnoli S, Sestili F, Palombieri S *et al.*, Boosting immunity and management against wheat *fusarium* diseases by a sustainable, circular nanostructured delivery platform. *Plan Theory* **12**:1223 (2023).
23 Botticella E, Sestili F, Sparla F, Moscatello S, Marri L, Cuesta-Seijo JA *et al.*, Combining mutations at genes encoding key enzymes involved in starch synthesis affects the amylose content, carbohydrate allocation and hardness in the wheat grain. *Plant Biotechnol J* **16**:1723–1734 (2018).
24 King EO, Ward MK and Raney DE, Two simple media for the demonstration of pyocyanin and fluorescin. *J Lab Clin Med* **44**:301–307 (1954).
25 Shao X, Xie Y, Zhang Y and Deng X, Biofilm formation assay in *pseudomonas syringae*. *Bio-Protocol* **9**:e3237 (2019).
26 Liu HH, Yang YR, Shen XC, Zhang ZL, Shen P and Xie ZX, Role of DNA in bacterial aggregation. *Curr Microbiol* **57**:139–144 (2008).
27 Noronha VT, Camargos CHM, Jackson JC, Souza Filho AG, Paula AJ, Rezende CA *et al.*, Physical membrane-stress-mediated antimicrobial properties of cellulose nanocrystals. *ACS Sustain Chem Eng* **9**:3203–3212 (2021).
28 Bustin SA, Benes V, Garson JA, Hellemans J, Huggett J, Kubista M *et al.*, The MIQE guidelines: minimum information for publication of quantitative real-time PCR experiments. *Clin Chem* **55**:611–622 (2009).
29 Metsalu T and Vilo J, ClustVis: a web tool for visualizing clustering of multivariate data using principal component analysis and heatmap. *Nucleic Acids Res* **43**:566–570 (2015).
30 Luzi F, Fortunati E, Giovanale G, Mazzaglia A, Torre L and Balestra GM, Cellulose nanocrystals from *Actinidia deliciosa* pruning residues combined with carvacrol in PVA_CH films with antioxidant/antimicrobial properties for packaging applications. *Int J Biol Macromol* **104**:43–55 (2017).
31 Fortunati E, Rescignano N, Botticella E, La Fiandra D, Renzi M, Mazzaglia A *et al.*, Effect of poly(DL-lactide-co-glycolide) nanoparticles or cellulose nanocrystals-based formulations on *pseudomonas syringae* pv. *Tomato* (Pst) and tomato plant development. *J Plant Dis Prot* **123**:301–310 (2016).
32 Schiavi D, Balbi R, Giovagnoli S, Camaioni E, Botticella E, Sestili F *et al.*, A green nanostructured pesticide to control tomato bacterial speck disease. *Nanomaterials* **11**:1852 (2021).
33 Maluin FN and Hussein MZ, Chitosan-based agronanochemicals as a sustainable alternative in crop protection. *Molecules* **25**:7 (2020).
34 Yu J, Wang D, Geetha N, Khawar KM, Jogaiah S and Mujtaba M, Current trends and challenges in the synthesis and applications of chitosan-based nanocomposites for plants: a review. *Carbohydr Polym* **261**:117904 (2021).
35 Kumaraswamy RV, Kumari S, Choudhary RC, Pal A, Raliya R, Biswas P *et al.*, Engineered chitosan based nanomaterials: bioactivities, mechanisms and perspectives in plant protection and growth. *Int J Biol Macromol* **113**:494–506 (2018).
36 Fortunati E, Giovanale G, Luzi F, Mazzaglia A, Kenny JM, Torre L *et al.*, Effective postharvest preservation of kiwifruit and romaine lettuce with a chitosan hydrochloride coating. *Coatings* **7**:196 (2017).
37 Ferrante P and Scortichini M, Molecular and phenotypic features of *pseudomonas syringae* pv. *Actinidiae* isolated during recent epidemics of bacterial canker on yellow kiwifruit (*Actinidia chinensis*) in Central Italy. *Plant Pathol* **59**:954–962 (2010).
38 Scortichini M, Field efficacy of chitosan to control *pseudomonas syringae* pv. *Actinidiae*, the causal agent of kiwifruit bacterial canker. *Eur J Plant Pathol* **140**:887–892 (2014).
39 Mansilla AY, Albertengo L, Rodríguez MS, Debbaudt A, Zúñiga A and Casalongué CA, Evidence on antimicrobial properties and mode of

Pest Management Science published by John Wiley & Sons Ltd on behalf of Society of Chemical Industry.

action of a chitosan obtained from crustacean exoskeletons on *pseudomonas syringae* pv. *Tomato* DC3000. *Appl Microbiol Biotechnol* **97**: 6957–6966 (2013).
40 Rossetti A, Mazzaglia A, Muganu M, Paolocci M, Sguizzato M, Esposito E *et al*., Microparticles containing gallic and ellagic acids for the biological control of bacterial diseases of kiwifruit plants. *J Plant Dis Prot* **124**:563–575 (2017).
41 Canzoniere P, Francesconi S, Giovando S and Balestra GM, Antibacterial activity of tannins towards *pseudomonas syringae* pv. *Tomato*, and their potential as biostimulant on tomato plants. *Phytopathol Mediterr* **60**:23–36 (2021).
42 Quattrucci A, Ovidi E, Tiezzi A, Vinciguerra V and Balestra GM, Biological control of tomato bacterial speck using *Punica granatum* fruit peel extract. *Crop Prot* **46**:18–22 (2013).
43 Pinto M, Soares C, Andreani T, Fidalgo F and Tavares F, *Eucalyptus globulus* leaf aqueous extract differentially inhibits the growth of three bacterial tomato pathogens. *Plan Theory* **12**:8 (2023).
44 Cortesi R, Quattrucci A, Esposito E, Mazzaglia A and Balestra GM, Natural antimicrobials in spray-dried microparticles based on cellulose derivatives as potential eco-compatible agrochemicals. *J Plant Dis Prot* **124**:269–278 (2017).
45 Pannucci E, Caracciolo R, Romani A, Cacciola F, Dugo P, Bernini R *et al*., An hydroxytyrosol enriched extract from olive mill wastewaters exerts antioxidant activity and antimicrobial activity on *pseudomonas savastanoi* pv. *Savastanoi* and *agrobacterium tumefaciens*. *Nat Prod Res* **35**:2677–2684 (2021).
46 Trigui M, Ben Hsouna A, Hammami I, Culioli G, Ksantini M, Tounsi S *et al*., Efficacy of *Lawsonia inermis* leaves extract and its phenolic compounds against olive knot and crown gall diseases. *Crop Prot* **45**:83–88 (2013).
47 Rafique M, Hayat K, Mukhtar T, Khan A, Afridi M, Hussain T *et al*., Bacterial biofilm formation and its role against agricultural pathogens, in *The Battle against Microbial Pathogens: Basic Science, Technological Advances and Educational Programs*, ed. by Villas AM. Spain, Formatex research Center, pp. 373–382 (2015).
48 Walsh DJ, Livinghouse T, Goeres DM, Mettler M and Stewart PS, Antimicrobial activity of naturally occurring phenols and derivatives against biofilm and planktonic bacteria. *Front Chem* **7**:653 (2019).
49 Mah TFC and O'Toole GA, Mechanisms of biofilm resistance to antimicrobial agents. *Trends Microbiol* **9**:34–39 (2001).
50 Castiblanco LF and Sundin GW, New insights on molecular regulation of biofilm formation in plant-associated bacteria. *J Integr Plant Biol* **58**:362–372 (2016).
51 Cellini A, Fiorentini L, Buriani G, Yu J, Donati I, Cornish DA *et al*., Elicitors of the salicylic acid pathway reduce incidence of bacterial canker of kiwifruit caused by *pseudomonas syringae* pv. *Actinidae*. *Ann Appl Biol* **165**:441–453 (2014).
52 Nunes da Silva M, SMP C, Rodrigues AM, Aurelio G-C, António C and Vasconcelos MW, Defence-related pathways, phytohormones and primary metabolism are key players in kiwifruit plant tolerance to *Pseudomonas syringae* pv. *Actinidiae*. *Plant Cell Environ* **45**:528–541 (2022).
53 Song Y, Sun L, Lin M, Chen J, Qi X, Hu C *et al*., Comparative transcriptome analysis of resistant and susceptible kiwifruits in response to *pseudomonas syringae* pv. *Actinidiae* during early infection. *PloS One* **14**:e0211913 (2019).
54 Corsi B, Huub LJM, Forni C and Riccioni L, Enhancement of *PR1* and *PR5* gene expressions by chitosan treatment in kiwifruit plants inoculated with *pseudomonas syringae* pv. *Actinidiae*. *Eur J Epidemiol* **148**:163–179 (2017).
55 Li Y, Wang X, Zeng Y and Liu P, Metabolic profiling reveals local and systemic responses of kiwifruit to *pseudomonas syringae* pv. *Actinidiae*. *Plant. Director* **4**:1–13 (2020).
56 Petriccione M, Salzano AM, Di Cecco I, Scaloni A and Scortichini M, Proteomic analysis of the *Actinidia deliciosa* leaf apoplast during biotrophic colonization by *pseudomonas syringae* pv. *Actinidiae*. *J Proteomics* **101**:43–62 (2014).
57 Qin X, Zhang M, Li Q, Chen D, Sun L, Qi X *et al*., Transcriptional analysis on resistant and susceptible kiwifruit genotypes activating different plant-immunity processes against *pseudomonas syringae* pv. *Actinidiae*. *Int J Mol Sci* **23**:14 (2022).
58 Wang T, Wang G, Jia ZH, Pan DL, Zhang JY and Guo ZR, Transcriptome analysis of kiwifruit in response to *pseudomonas syringae* pv. *Actinidiae* infection. *Int J Mol Sci* **19**:2 (2018).
59 Jones DH, Phenylalanine ammonia-lyase: regulation of its induction, and its role in plant development. *Phytochemistry* **23**:1349–1359 (1984).
60 Gao S, Yan R, Cao M, Yang W, Wang S and Chen F, Effects of copper on growth, antioxidant enzymes and phenylalanine ammonia-lyase activities in *Jatropha curcas* L. seedling. *Plant Soil Environ* **54**:117–122 (2008).
61 Aziz A, Trotel-Aziz P, Dhuicq L, Jeandet P, Couderchet M and Vernet G, Chitosan oligomers and copper sulfate induce grapevine defense reactions and resistance to gray mold and downy mildew. *Phytopathology* **96**:1188–1194 (2006).
62 Jia X, Zeng H, Wang W, Zhang F and Yin H, Chitosan oligosaccharide induces resistance to *pseudomonas syringae* pv. *Tomato* DC3000 in *Arabidopsis thaliana* by activating both salicylic acid– and jasmonic acid–mediated pathways. *Mol Plant Microbe Interact* **31**:1271–1279 (2018).
63 García-Sánchez M, Garrido I, de Casimiro I J, Casero PJ, Espinosa F, García-Romera I *et al*., Defence response of tomato seedlings to oxidative stress induced by phenolic compounds from dry olive mill residue. *Chemosphere* **89**:708–716 (2012).
64 El-Nagar A, Elzaawely AA, Taha NA and Nehela Y, The antifungal activity of gallic acid and its derivatives against *Alternaria solani*, the causal agent of tomato early blight. *Agronomy* **10**:1402 (2020).
65 Mohamed MDA, Moharam MHA and Ahmed HAM, *In vitro* and *in vivo* toxicity of nano chitosan against *Curvularia lunata*, the causal microorganism of fruit rot and blight, a new disease of olive (*O. Europaea* L.). *Eur J Plant Pathol* **161**:881–894 (2021).
66 Aitouguinane M, El A-TZ, Rchid H, Fendri I, Abdelkafi S, El-Hadj MDO *et al*., Polysaccharides from moroccan green and brown seaweed and their derivatives stimulate natural defenses in olive tree leaves. *Appl Sci* **12**:17 (2022).
67 Barrett-Manako K, Andersen M, Martínez-Sánchez M, Jenkins H, Hunter S, Reese-George J *et al*., Real-time PCR and droplet digital PCR are accurate and reliable methods to quantify *pseudomonas syringae* pv. *Actinidiae* biovar 3 in kiwifruit infected plantlets. *Plant Dis* **105**:1748–1757 (2021).
68 Gallelli A, Talocci S, Pilotti M and Loreti S, Real-time and qualitative PCR for detecting *pseudomonas syringae* pv. *Actinidiae* isolates causing recent outbreaks of kiwifruit bacterial canker. *Plant Pathol* **63**:264–276 (2014).
69 Donati I, Cellini A, Buriani G, Mauri S, Kay C, Tacconi G *et al*., Pathways of flower infection and pollen-mediated dispersion of *pseudomonas syringae* pv. *Actinidiae*, the causal agent of kiwifruit bacterial canker. *Hortic Res* **5**:1 (2018).
70 Chai AL, Ben HY, Guo WT, Shi YX, Xie XW, Li L *et al*., Quantification of viable cells of *pseudomonas syringae* pv. *Tomato* in tomato seed using propidium monoazide and a real-time PCR assay. *Plant Dis* **104**:2225–2232 (2020).
71 Fanelli V, Cariddi C and Finetti-Sialer M, Selective detection of *pseudomonas syringae* pv. *Tomato* using dot blot hybridization and real-time PCR. *Plant Pathol* **56**:683–691 (2007).
72 Tegli S, Cerboneschi M, Libelli IM and Santilli E, Development of a versatile tool for the simultaneous differential detection of *pseudomonas savastanoi* pathovars by end point and real-time PCR. *BMC Microbiol* **10**:1–14 (2010).

